JOURNAL OF GEOPHYSICAL RESEARCH, VOL. 107, NO. A9, 1234, doi:10.1029/2001JA000313, 2002

Properties of magnetic clouds and geomagnetic storms associated with eruption of coronal sigmoids

Robert J. Leamon and Richard C. Canfield
Department of Physics, Montana State University, Bozeman, Montana, USA

Alexei A. Pevtsov
National Solar Observatory/Sacramento Peak, Sunspot, New Mexico, USA

Received 25 September 2001; revised 18 January 2002; accepted 18 January 2002; published 12 September 2002.

[1] We study 46 solar coronal eruptions associated with sigmoids seen in images from the Yohkoh Soft X-ray Telescope (SXT). We relate the properties of the sigmoids to in situ measurements at 1 AU and geomagnetic storms. Our primary result is that erupting sigmoids tend to produce geoeffective magnetic clouds (MCs): 85% of the erupting sigmoidal structures studied spawned at least a "moderate" ($|Dst| \geq 50$ nT) geomagnetic storm. A collateral result is that MCs associated with sigmoids do not show the same solar-terrestrial correlations as those associated with filaments and, as such, form a distinct class of events. First, rather than reversing with the global solar dipole (at solar maximum), the leading field in MCs weakly (2:1) shows a solar cycle (Hale polarity) based correlation (reversing at solar minimum). Second, whereas the handedness of MCs associated with filament eruptions is strongly (95%) related to their launch hemisphere, that of MCs associated with sigmoid eruptions is only weakly (~70%) so related. Finally, we are unaware of any model of the magnetic fields of sigmoids and their eruption that gives a useful prediction of the leading field orientation of their associated MC. *INDEX TERMS:* 2111 Interplanetary Physics: Ejecta, driver gases, and magnetic clouds; 2784 Magnetospheric Physics: Solar wind/magnetosphere interactions; 7509 Solar Physics, Astrophysics, and Astronomy: Corona; 7513 Solar Physics, Astrophysics, and Astronomy: Coronal mass ejections; *KEYWORDS:* sigmoids, coronal mass ejections, magnetic clouds, Sun-Earth interactions, magnetic storms

Citation: Leamon, R. J., R. C. Canfield, and A. A. Pevtsov, Properties of magnetic clouds and geomagnetic storms associated with eruption of coronal sigmoids, *J. Geophys. Res.*, *107*(A9), 1234, doi:10.1029/2001JA000313, 2002.

1. Introduction

[2] Large-scale helical magnetic structures, commonly called magnetic clouds (MCs), are observed as the interplanetary consequence of solar coronal mass ejections (CMEs). A significant fraction of all CMEs directed toward earth (at least one-third [*Gosling*, 1990], perhaps considerably more [*Lepping and Berdichevsky*, 2000]), are associated with MCs. Numerous studies carried out over the last two decades have implicated the prolonged southward component of the interplanetary magnetic field (IMF) associated with MCs in major geomagnetic storms [e.g., *Gonzalez and Tsurutani*, 1987]. *Lepping and Berdichevsky* [2000] have recently reviewed the sources, properties, models, and geomagnetic relationships of MCs. The helical "magnetic flux rope" structure of MCs is readily identified in interplanetary data from its enhanced field strength and smooth and slow variation (over ~one day) of field direction as the cloud sweeps by a given spacecraft [*Burlaga et al.*, 1981]. It is clear that the solar sources of MCs are CMEs [e.g., *Shimazu and Marubashi*, 2000], which in turn originate in association with filament eruptions (typically not associated with active regions) and eruptive flares (typically associated with active regions). The 3-D magnetic models and geomagnetic relationships are much better understood for filament eruptions than for active region phenomena.

[3] Solar filaments, which are observed in Hα and EUV images, are a manifestation of helical magnetic fields. The interpretation of these observations has been controversial [cf. *Rust*, 1997; *Martin and McAllister*, 1997]. However, independent evidence comparing models with observations [e.g., *Aulanier and Démoulin*, 1998; *Aulanier et al.*, 1998] strongly favors an interpretation in terms of primarily horizontal helical field lines whose upward-concave regions support filament material. Filaments are segregated in hemisphere by a strong hemispheric handedness rule [*Martin et al.*, 1994]. The topology implied by the models of Aulanier and colleagues is left-handed in the Northern Hemisphere and right-handed in the Southern Hemisphere.

[4] *Rust* [2001] reviews several aspects of the formation, magnetic structure, and eruption of filaments that are central

0148-0227/02/2001JA000313$09.00

to this paper. Those filaments typically associated with CMEs are so-called polar crown filaments and others that are not directly (and perhaps not even indirectly) associated with solar active regions. The axial magnetic fields of these filaments show a systematic dependence on the solar cycle. Unlike active regions, their typical axial magnetic field direction tends to reverse at solar maximum. For example, in the years leading up to sunspot maximum in even-numbered cycles, the magnetic field vectors in polar crown filaments point predominantly westward in the Northern Hemisphere and eastward in the Southern Hemisphere. The correlation of the handedness of magnetic clouds with the hemisphere of erupting filaments has been established quite clearly [*Marubashi*, 1986; *Bothmer and Schwenn*, 1994; *Rust and Kumar*, 1994]. Those erupting from the Northern Hemisphere are almost invariably left-handed, and those from the Southern Hemisphere, right-handed, and this pattern is the same for both odd- and even-numbered cycles [*Bothmer and Rust*, 1997].

[5] SOHO and Yohkoh observations of halo CMEs have led to the realization that the regions from which many CMEs are launched have sinuous S or inverse-S (sigmoidal) X-ray structure [*Sterling and Hudson*, 1997; *Hudson et al.*, 1998; *Canfield et al.*, 1999]. Though sigmoids are undoubtedly comprised of twisted fields, there are currently many competing topological models [cf. *Rust and Kumar*, 1996; *Pevtsov et al.*, 1996; *Titov and Démoulin*, 1999; *Amari and Luciani*, 1999; *Gibson and Low*, 2001].

[6] For convenience, we use the coronal flux rope (CFR) model of *Pevtsov and Canfield* [2001] as a point of reference for our analyses in this paper. It does not matter which one of these models we take, since all of them result in a dichotomous prediction of the out-of-ecliptic IMF component (see section 4.2, below). In this CFR model, a toroidal flux rope is embedded in an overlying dipolar flux system. The projected magnetic separatrix surfaces are sigmoidal: S-shaped when the flux rope is right-handed, and S structures when it is left-handed [*Titov and Démoulin*, 1999]. Our use of this model assumes that the embedded coronal flux rope becomes the flux rope of the magnetic cloud. Although this assumption is far from proven, it makes a useful hypothesis to test in the present paper, and is not intended to support one or another of the competing models.

[7] *Canfield et al.* [2000] review models of sigmoids, as well as the characteristics of the ''sigmoid to arcade'' signatures in Yohkoh soft X-ray images that reveals their eruptions. These authors show that the hemispheric handedness relationship for sigmoids and active regions is much weaker than that for filaments—only about 60–70% of sigmoids (active regions) have the handedness typical of their hemisphere. Like filaments, this hemispheric handedness ''rule'' does not change from one cycle to the next *Pevtsov et al.* [2001]. However, the east-west component of the magnetic field (often identified with the polarity of the leading sunspot) of active regions, unlike filaments, reverses at sunspot minimum, i.e., between one numbered cycle and the next [*Hale and Nicholson*, 1938].

[8] Other studies are presently underway with much broader goals than ours, for example, to determine the 3-D magnetic structure and topology of active regions, to understand how filaments and sigmoids are formed and what topological features lead to their eruption. In this paper we have a much narrower focus—we ask how the observed properties of sigmoidal regions in the corona are related to associated interplanetary magnetic clouds and geomagnetic storms. In section 2 we detail our basic data set of magnetic clouds and geomagnetic storms related to X-ray sigmoids eruptions, and in section 3 we describe our methods of determination of coronal and geophysical parameters. In section 4 we explore relationships between solar, interplanetary, and geophysical parameters, including some limited predictions of the geomagnetic storm indices. The solar-terrestrial correlations shown suggest that there are differences between CMEs spawned in sigmoid-associated eruptions and those related to quiescent filament disappearances. We discuss this in section 5, before summarizing our results, the applicability and limits of our approach, and some suggestions for future research directions.

2. Data Selection

[9] We combine 4 previously existing databases for events to be studied here. These data sets are disparate in their observational parameters: none include all the parameters required for this study, and we extend them accordingly, as discussed below. Table 1 lists all the events studied and their properties and identifies, in the first column, the database of origin:

1. *Pevtsov and Canfield* [2001] studied 19 eruptions of coronal sigmoids (labeled P1–P19) that were temporally correlated with geomagnetic storms (enhanced *Ap* index). They used the sigmoid to arcade signatures used by *Canfield et al.* [1999] to identify eruptions in the Yohkoh data; we adopt the same criterion to identify erupting sigmoids in the present paper. We can find a clearly identifiable (flux rope) magnetic cloud in the in situ data in all but 5 of these events. However, we include all 19 events in Table 1 because in having *Ap* (and *Dst*) data for these 5 events we can study the geomagnetic consequences of the sigmoid eruption.

The solar source times listed in Table 1 are times of specific Yohkoh SXT images that first show signs of eruption. One has to bear in mind that SXT images are not sampled in a uniform manner. However, time uncertainty of a few minutes (or even a few hours) is not critical for the present study. For this reason, we also only cite the first sigmoid brightening of those *Pevtsov and Canfield* [2001] events that had multiple brightenings or eruptions related to only one event (geomagnetic storm or flux rope) at 1 AU.

2. *Gopalswamy et al.* [2000] studied 28 interplanetary ejecta events from Wind of identifiable solar origin (by SOHO/LASCO), of which 20 had flux-rope structure. *Gopalswamy et al.* list the solar source of each of their events, determined from SXT or SOHO/EIT and synoptic data ''to eliminate backside events.'' It is therefore easy to apply the sigmoid to arcade criterion to the events at the given location and time. Evidence of a sigmoid eruption is absent in only 3 of *Gopalswamy et al.*'s events, one of which occurred during several days of Yohkoh down-time. The interplanetary ejecta resulting from the December 16, 1997, 0230 UT event (*Gopalswamy et al.*'s No. 19) did not have a flux-rope structure. Having neither an observable sigmoid or flux rope, we exclude this event from further study here, leaving a total of 19 events from this database. We keep the numbering system of *Gopalswamy et al.* prepending the

Table 1. Eruptions From Sigmoids

Eruption Number[a]	Solar Source Date (UT)	Orientation (CFR Model)	Shape	NOAA AR	*Ap* Index (Peak)	Flux Rope Handedness	Initial Field Direction	Density Enh? Front/Rear
P1	1991/10/14 20:43	N	S	none	18	L	N	F
P2	1991/12/26 17:08	N	S	6982 (S16W15)	94	...	...	...
P3	1992/02/06 09:34	N	S	7042 (S15EW0)	132	R	S	F
P4	1992/03/16 20:07	N	S	7100 (S15E01)	48	...	...	...
P5	1992/03/29 22:13	N	N	7117 (N13E08)	27	L	S	F
P6	1992/04/08 08:19	N	S	7123 (S07W09)	9	R	N	...
P7	1992/05/08 15:04	S	N	7154 (S27E14)	300	R	N	...
P8	1992/06/17 14:42	N	S	7194 (S07W11)	94	L	N	F
P9	1992/10/04 09:47	N	S	none	22	R	N	R
P10	1992/10/22 07:42	N	N	7315 (N01W10)	48	...	...	...
P11	1992/10/22 15:35	N	S	7316 (S15E30)	48	L	S	F
P12	1992/11/28 20:39	N	N	7348 (N13E01)	39	...	...	...
P13	1992/12/24 04:20	N	S	7374 (S10W19)	94	R	N	F
C1	1993/03/05 02:39	S	S	7443 (N15W35)	111	L	N	F
C2	1993/07/31 09:35	N	N	7552 (N17W22)	56	L	S	F
C3	1993/12/01 06:03	S	S	7624 (N03W19)	111	L	S	F
P14	1994/10/19 22:55	N	N	7790 (N12W24)	94	...	...	...
P15	1994/10/25 10:00	S	N	7792 (S09W12)	132	R	N	F
W1	1995/02/04 16:02	N	S	7834 (S07E12)	9	L	S	F + R
W2	1995/02/28 08:46	N	S	7846 (S16E43)	39	L	N	F
W3	1995/12/11 02:24	N	S	7930 (S10W25)	18	L	S	F
P16	1996/12/19 14:06	N	S	8005 (S13W10)	22	R	N	F + R
G2	1997/01/06 15:10[b]	S	S	none (S18E06)	80	R	S	R
G3	1997/02/07 00:30	S	S	8016 (S20W45)	67	...	...	...
P17	1997/04/07 13:29	S	S	8027 (S29E22)	111	R	N	F
G5	1997/04/16 07:35	S	S	8032 (S22E04)	56	R	S	F + R
P18	1997/05/12 05:22	S	N	8038 (N22W14)	111	L	S	F
G7	1997/06/05 22:55	S	S	8048 (S35W17)	67	R	S	...
C4	1997/07/05 16:41	S	S	8059 (S30W15)	27	R	S	R
G10	1997/07/30 04:45	S	N	8066 (N45E21)	48	L	S	F
G11	1997/08/30 01:30	N	S	8076 (N30E17)	94	R	N	F + R
G13	1997/09/17 20:28	N	S	none (N30W35)	48	L	N[c]	F
G14	1997/09/28 01:08	S	N	none (N22E05)	132	L	N[c]	...
G15	1997/10/06 15:28	S	S	none (S54E46?)	94	R	N	F
G16	1997/11/04 06:10	S	S	8100 (S14W33)	132	R	S	F
G17	1997/11/19 12:26	N	S	8108 (N19W03)	154	R	S[c]	F
G18	1997/12/06 10:27	S	N	8113 (N47W13)	27	L	N	...
G20	1998/01/02 23:28	...[d]	...[d]	none (N47W03)	94	L	S	R
G23	1998/02/14 07:00	N	N	8156 (S26E35)	111	R	S	...
G24	1998/02/28 12:48	...	...	8171 (S24W01)	48	L	S	R
G25	1998/04/29 16:58	N	S	8210 (S18E20)	300	...	...	...
G26	1998/05/02 14:06	N	S	8210 (S15W15)	300	...	...	...
G27	1998/05/31 04:26	N	S	8227 (N28E09)	32	L	S	F
G28	1998/06/21 05:35	N	S	8243 (N16W38)	94	L	N[c]	F
P19	1998/11/09 17:41	S	S	8378? (N20W02)	80	R	N	F + R
L1	2000/10/25 16:55	S	N	9201 (N14W21)	80	L	S	...

[a] Events P1–P19 are from *Pevtsov and Canfield* [2001]; events G2–G28 are from *Gopalswamy et al.* [2000]; events C1–C7 are from *Canfield et al.* [1999]; events W1–W3 are from the WIND online database; and event L1 is unique to this study.
[b] Sigmoid brightening only; see text.
[c] Field always in this direction; flux rope is perpendicular to ecliptic.
[d] No Yohkoh data for 5 days encompassing this period.

letter "G"; however, 3 of the 20 events on *Gopalswamy et al.*'s list that showed evidence of an erupting sigmoid overlapped with *Pevtsov and Canfield*'s data. Those 3 events present in both the *Pevtsov and Canfield* and *Gopalswamy et al.* lists appear in Table 1 as "P" events only: G1 is the same as P16, G4 is P17 and G6 is P18.

3. *Canfield et al.* [1999] observed 61 eruptive active regions during 1993 and 1997. Searching this database for sigmoid events that spawned flux rope magnetic clouds not covered by either of the above two databases finds 4 more events that show an unambiguous erupting sigmoid signature. These are labelled C1–C4 in Table 1.

4. Table 1 also includes three of the seven pre-solar minimum magnetic clouds collected by the Wind/MFI team (available online at http://lepmfi.gsfc.nasa.gov/mfi/mag_cloud_pub1.html) that were not included in any of the above three lists and could unambiguously be associated with eruption of a coronal sigmoid. These events, labeled W1–W3, were included to improve the sampling statistics of cycle 22 versus those of cycle 23 because Wind and ACE were not launched until several years after Yohkoh. As a result of this poorer temporal coverage of interplanetary data, five events from *Pevtsov and Canfield* [2001] in Table 1 have no definite magnetic cloud association. The same problem limits the search of *Canfield et al.* [1999] events from 1993.

[10] Finally, we add one event unique to the present data set (L1, October 25, 2000). This was selected because it was the first major eruption after the start of the present project,

and that the resulting storm enabled one of us (RJL) to see the aurora borealis for the first time.

[11] In total, then, we have investigated 46 eruptions seen in Yohkoh SXT images listed in Table 1. Of these, we are unable to identify a helical flux rope in the IMF data in only 8 cases and cannot unambiguously resolve a sigmoidal active region in only 2 of the cases originally selected from their interplanetary signatures or a white-light CME.

[12] Due to the disparate nature of the data sets, we need to uniformly relate one sigmoid eruption with one interplanetary magnetic cloud. To do so, we calculate the difference between the "constant velocity transit" (147 million km divided by the solar wind speed observed in the interplanetary ejecta) and the observed transit time for all of the *Gopalswamy et al.* [2000] events. The average deviation is 9.4 ± 14.4 hours (i.e., cloud arrived before constant velocity prediction). From this, we exclude events from the other data sets where there are two (or more) possible sources that erupted within less than a day of one another for one interplanetary flux rope.

[13] Several events in the two data sets originating with X-ray images had other indications of solar ejecta, such as enhanced Helium abundance, enhanced α/p ratio, or bi-directional electron streaming [e.g., *Gosling*, 1996; *Larson et al.*, 1997], but a magnetic cloud could not clearly be identified. Eight such events appear in Table 1, but, of course, are not used in the correlation studies of cloud properties.

[14] We have kept event G2 in the database even though the sigmoid does not exhibit the eruption criteria applied in the selection of other events in this study. Rather it merely brightens, with its X-ray intensity peaking at 1510UT, and remains sigmoidal afterwards. This is the much-studied January 1997 event (see *Burlaga et al.* [1998], *Webb et al.* [1998], and the special issue of *Geophysical Research Letters*, volume 25, number 14). Much has been discussed on the lack of chromospheric, coronal, or X-ray activity prior to the CME. Given the occurrence of a sigmoid brightening and the obvious interest in this event, we have included it in this study.

3. Parameters Inferred From Data

[15] We keep track of 6 dichotomous variables for each event determined as follows:

1. Sigmoid shape (S or inverse-S in Yohkoh SXT images, column 4 in Table 1).

2. Sigmoid eruption hemisphere (north or south, column 5 in Table 1).

3. Leading field predicted by CFR model (north or south, column 3 in Table 1).

To designate a given active region as N-CFR or S-CFR, we look at the underlying dipole in a photospheric line-of-sight magnetogram. The leading sunspot has either positive or negative flux. We combine this with the sigmoid shape, which implies either a left- or right-handed coronal flux rope. Pointing the thumb of one's appropriate hand from positive to negative flux, the direction of the curled fingers reveals whether the outer (i.e., highest in the corona) coils of the coronal flux rope are northwards- or southwards-pointing. The positive and negative flux regions in the magnetogram might be more closely aligned north-south than east-west, implying a leading field more east-west, but it is only the projected component 'N' or 'S' that appears in column 3 of Table 1.

We admit the possibility that the axial field direction in the sigmoids cannot be determined from the polarity of the leader spot in a simple way; AR sigmoids do not necessarily connect the leader and follower polarities in a straightforward way.

4. Leading field direction as observed (north or south, column 8 in Table 1).

5. Handedness of flux rope as observed in situ (left- or right-handed, column 7 in Table 1).

Both leading magnetic field and handedness are easily determined by looking at the IMF data. Table 2 succinctly summarizes the bimodal relation between the evolution of field latitude and longitude in conventional RTN coordinates and the handedness of the flux rope. A few clouds rotated in a unipolar sense perpendicular to the ecliptic and these are footnoted in Table 1. We use Table 2 of *Mulligan et al.* [1998] to ascertain the handedness of such clouds, (e.g., east−north−west or west−south−east for a left-handed cloud).

Table 2. Determination of Magnetic Cloud Handedness

	Longitude, Φ	
Latitude, θ	<180°	>180°
+ → −	R	L
− → +	L	R

6. Solar cycle: 22 or 23.

We split our data set into solar cycle 22 and solar cycle 23 observations, either side of solar minimum, where the leading polarity of active regions reverses (the Hale cycle [*Hale and Nicholson*, 1938]). A few events occurred when there were active regions from both "old" and "new" cycles, but their cycle association can be based on their polarity and latitude [see, e.g., *Webb et al.*, 2000a, Table 1]. There is no overlap in the present data set, however, and all events before December 31, 1996 are in cycle 22 and all events after January 1, 1997 are in cycle 23.

[16] As an example of how these parameters are determined, we use the May 1997 event, studied in detail by *Webb et al.* [2000b] and shown in Figures 1 and 2. First we examine the solar data. In Figure 1, an inverse-S (left-handed) sigmoid in the Northern Hemisphere erupts. To infer the leading field predicted by the CFR model, we combine the fact that the sigmoid is inverse-S (so the flux rope is left-handed, in agreement with *Webb et al.*'s inference from the filament structure) with the polarity structure of the active region given by a magnetogram. The leading sunspot polarity for AR 8038 was positive. Therefore, the predicted leading magnetic field of the modeled coronal flux rope was southwards.

[17] Turning to interplanetary data, we see in Figure 2 that the latitude θ increases from almost $-90°$ (i.e., a southwards leading field) to $+45°$, while the longitude ϕ remains steady at $\sim 100°$. Looking at Table 2 tells us that this cloud is thus left-handed. This simple procedure is all that is necessary to ensure agreement with the more complete analysis of *Webb et al.*, who modeled the flux rope using the 7-parameter fit of *Lepping et al.* [1990] to the force-free field equation $\nabla \times \mathbf{B} = \alpha \mathbf{B}$.

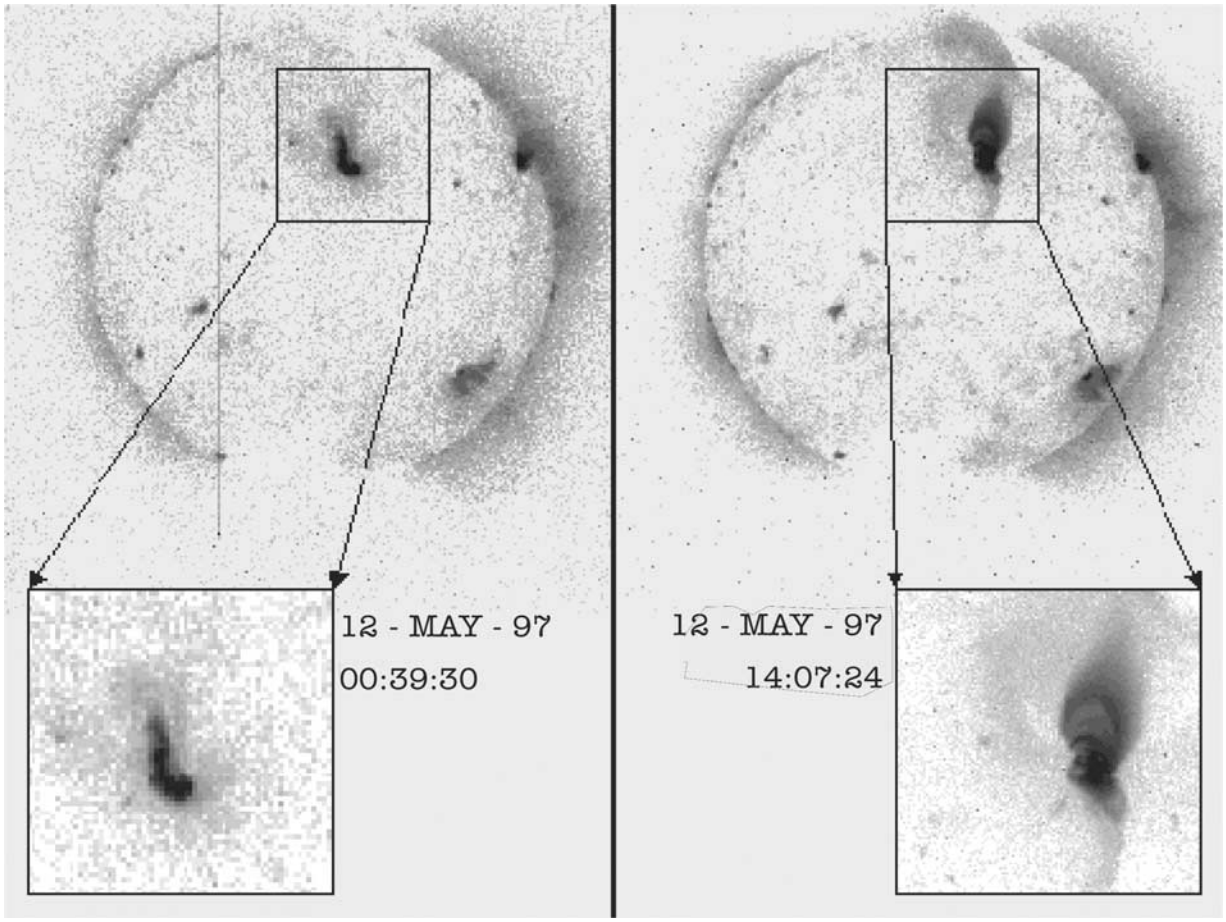

Figure 1. Illustration of the "sigmoid → arcade" morphology, in which a sigmoidal coronal structure above AR 8038 (left insert, 12-MAY-97 00:39:30 UT) erupts, leaving behind an arcade and a cusp (right insert, 12-MAY-97 14:07:24 UT). The interplanetary manifestation of this eruption is seen in Figure 2.

[18] We also track the average solar wind speed (V_{SW}) of the magnetic cloud, the *Ap* and *Dst* indices of the ensuing magnetic storms, and (qualitatively) whether there was a leading or trailing (or both) density enhancement.

4. Results

[19] In this section we analyze the relationships between the parameters of our study, deferring interpretation to section 5.

4.1. Launch Hemisphere Correlations

[20] The three 2 × 2 contingency tables seen in Table 3 show the number of events that are launched from each hemisphere and the handedness of the magnetic cloud they spawn. The first table corresponds to all our events, with the second and third corresponding to the cycle 22 and cycle 23 subsets, respectively. Using a χ^2 probability test based on Cramer's ϕ coefficient [*Press et al.*, 1992] on all the data, we can reject the null hypothesis (no association of hemisphere and handedness) with over 99% confidence. Northern Hemisphere eruptions spawn left-handed clouds in 13 of 16 (82%) cases, and Southern Hemisphere eruptions spawn right-handed clouds in 14 of 20 (70%) cases. These results are comparable to the findings of *Pevtsov et al.* [1995], i.e., the photospheric magnetic fields of only 76% of active regions in the Northern Hemisphere have negative current helicity, and only 69% in the Southern Hemisphere have positive current helicity.

[21] Shifting our attention to the periods before and after solar minimum (second and third contingency tables in Table 3), the null hypothesis can be rejected at 94% and >99% confidence for solar cycles 22 and 23, respectively. The same correlations between Northern Hemisphere and left-handed clouds and Southern Hemisphere and right-handed clouds exist before and after active region polarity reversal at solar minimum.

[22] Table 3 has the strongest correlation of any of the pairings studied. However, at "only" a 3:1 ratio, it is not as strong as the hemisphere–handedness correlation observed by *Bothmer and Rust* [1997], who found that only 1 of their 28 disappearing filament-associated events violated this rule. We shall return to discuss this further in section 5.1.

[23] Table 4 is another set of three contingency tables showing the relationship between hemisphere of eruption and the out-of-ecliptic IMF component of the leading part of the ensuing magnetic cloud. In cycle 22, we see an anti-correlation; by a 2:1 ratio, Southern Hemisphere events are correlated with northwards leading fields and vice-versa. Using the χ^2 test, we can reject the null hypothesis at the 82% confidence level. In cycle 23, on the other hand, at an

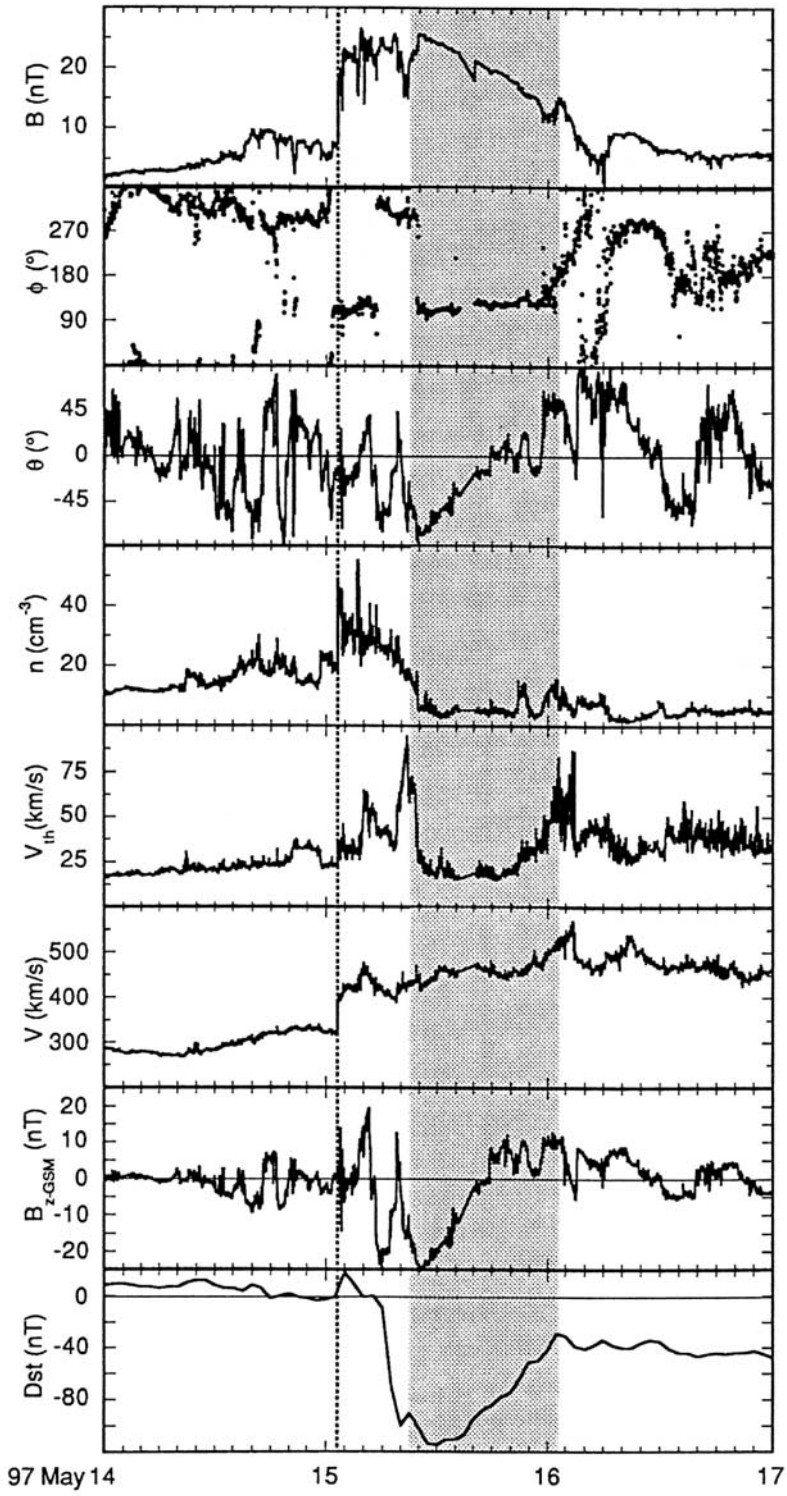

Figure 2. A typical magnetic cloud observed in the solar wind at 1 AU by WIND, due to the eruption shown in Figure 1 (Event P18 in Table 1). The vertical dashed line is the time of shock arrival and the shaded area denotes the boundaries of the flux rope as modeled by the WIND/MFI team. From *Webb et al.* [2002a], by permission.

Table 3. Launch Hemisphere Versus MC Flux Rope Handedness

	Total		Cycle 22		Cycle 23	
Launch Hemisphere	L	R	L	R	L	R
N	13	3	4	0	9	3
S	6	14	5	6	1	8

81% confidence level there is a positive association (i.e., Northern Hemisphere events are correlated with northwards leading fields) at a 1.6:1 ratio.

4.2. Sigmoid Shape and CFR Model Correlations

[24] Turning to the orientation properties of the sigmoids, Table 5 also shows a reversal at solar minimum in the association between the predicted direction of the outer coils of the sigmoidal coronal flux rope (from the CFR model) and the observed leading IMF component. Looking at the columns of Table 5, we can again clearly see the reversal of leading field direction at solar minimum, and looking at the rows we see a preponderance of northwards CFR model fields before minimum and a preference of southwards CFR fields after solar minimum. The results in Table 5 show that the CFR model predicts the correct leading IMF only 50% of the time. The same low success rate would be obtained for any of the models discussed in the introduction, even though the specific sign prediction might be opposite.

[25] Recall from section sec:method that the CFR model field is generated from the sigmoid shape and the underlying leading sunspot polarity. It is not surprising to see the CFR field direction preference reverse at solar minimum, since the association between hemisphere and sigmoid shape doesn't depend on solar cycle, whereas the sunspot polarity does reverse at solar minimum, as discussed in section 1.

[26] Our final correlation result is that between sigmoid shape and handedness of the MC flux rope, shown in Table 6. Here again, we see the correlation properties reverse at solar minimum, but the result is not as strong. Overall, there is a positive correlation between S-shaped sigmoids and right-handed flux ropes, at an 86% confidence level. In solar cycle 23, the positive correlation is at 98% confidence; in solar cycle 22, we have an anti-correlation with 32% confidence. This is not a high level of significance; however, Fisher's Exact Test [e.g., *Mehta and Patel*, 1983] says that there is only a 6% chance that the results of the two solar cycles come from the same parent distribution. In other words, there is a less than 10% chance that there is one correlation law between sigmoids and interplanetary clouds that exists for the whole 22 year solar cycle.

4.3. Sigmoids and Magnetic Storm Indices

[27] One of the original goals of the present study was to determine whether one might be able to predict, based on coronal or photospheric observations, whether a certain earth-directed CME from a sigmoidal region would produce a magnetic storm more or less significant than average, and, as such, offer useful information about an impending storm.

[28] Our primary result is that an erupting coronal sigmoid tends to produce at least a "moderate" geomagnetic storm. In our database, all storms have $|Dst| \geq 30$ nT and $Ap \geq 18$. Only 6 (16%) of sigmoid related events for which *Dst* was recorded had a value ≤ 50 nT, the definition of the onset of a "moderate" storm.

[29] For all dichotomous variables we have considered (launch hemisphere, sigmoid shape, flux rope handedness, etc.), we find no statistical significance that suggests that a given value of any of the variables we have studied gives rise to larger *Ap* or *Dst* indices. The largest difference between variables is that of leading field, where $\langle Dst \rangle_S = 76.8 \pm 32.2$ and $\langle Dst \rangle_N = 105.2 \pm 54.9$, with 18 and 17 events in each class, respectively. The difference between right- and left-handed flux ropes was almost as large. The fact that there is no statistically significant dependence on the leading field and not support for the "leading southwards fields generate stronger storms" paradigm [e.g., *Tsurutani and Gonzalez*, 1997], is curious but not compelling.

Table 5. CFR Model Leading Field Versus Observed IMF Direction

	Total		Cycle 22		Cycle 23	
CFR Field	N	S	N	S	N	S
N	10	10	7	6	3	4
S	8	8	3	1	5	7

5. Discussion and Summary

5.1. Sigmoid Eruptions and Quiescent Filament Disappearances

[30] We may consider all 67 events published in *Bothmer and Rust* [1997] in considering properties of the leading field of magnetic clouds. This database spans 28 years (from 1965 to 1993) and parts of solar cycles 20 and 22 and all of cycle 21. Twenty-eight events (from 1965 to 1980) list the solar location and magnetic polarity of an associated disappearing filament. There are two significant differences between the properties of sigmoid-associated eruptions described above and those of sudden filament disappearances, as studied by *Bothmer and Rust*:

1. The strongest correlation observed in the present work is between launch hemisphere and cloud handedness, at only a 3:1 ratio. This is an order of magnitude weaker than the rule for filament-associated events in *Bothmer and Rust*'s database: only one of their 28 events disobeys this hemisphere–handedness rule.

2. The leading field of sigmoid-related flux ropes does not follow that of the large-scale solar dipole. Several

Table 4. Launch Hemisphere Versus Leading IMF (*z*-Component) Direction

	Total		Cycle 22		Cycle 23	
Launch Hemisphere	N	S	N	S	N	S
N	7	9	1	3	6	6
S	9	11	7	4	2	7

Table 6. Erupting Sigmoid Shape Versus MC Flux Rope Handedness

	Total		Cycle 22		Cycle 23	
Sigmoid Shape	L	R	L	R	L	R
N	7	3	2	2	5	1
S	12	16	8	5	3	10

authors [e.g., *Mulligan et al.*, 2000; *Crooker*, 2000] view eruptions as non-local events, because the leading field direction of magnetic clouds tends to follow that of the large-scale solar dipole, reversing at solar maximum. On the other hand other authors [*Bothmer and Rust*, 1997; *Bothmer and Schwenn*, 1998] view eruptions as a local events, with IMF orientations correlating with the solar dipole only because the toroidal fields in filaments do so.

[31] In any case, there is a correlation between the solar dipole orientation and cloud leading field confirmed at a 4:1 margin in *Bothmer and Rust* and also by *Mulligan et al.* [1998]. However, *Bothmer and Rust*'s database comprised eruptions primarily from filament disappearances (''disparitions brusques'') outside active regions and often at higher solar latitudes than the active region belt. In contrast, summing the columns of Table 4, which includes only 6 eruptions from sites not assigned active region numbers by NOAA, we have only 20 of 36 (56%) events with southwards leading IMF, and for the entire Yohkoh mission thus far, the solar dipole has been southwards.

[32] In summary, neither a local model (represented here by the CFR model) nor a large-scale solar dipole model succeeds in accurately predicting the observed leading IMF of magnetic clouds from the solar properties of sigmoid eruptions. It is possible that large-scale writhing (almost 180°) of the coronal flux rope axis occurs in the course of eruption, which is going to invalidate simplistic predictions of leading field from self-similar expansion of a coronal flux rope. *Webb et al.* [2000b] note that the axis of the magnetic cloud from the May 1997 event passed slightly below the ecliptic plane, whereas the source was north of the solar equator (at N22E14). In Hα images, they observed that part of the erupting filament was moving towards the solar equator and rotating towards alignment with it. However, this is the only filament rotation immediately prior to disappearance or eruption seen with SOHO/EIT (S.P. Plunkett, private communication, 2001), which would seem to refute the large-scale writhing hypothesis.

5.2. Conclusions

[33] We have investigated the properties of coronal mass ejections associated with eruption of coronal sigmoids and their resulting interplanetary ejecta in terms of their solar cycle variation. We have four key results:

1. An erupting sigmoid will, most likely, produce a flux rope structure in interplanetary space, and upon impacting the Earth's magnetosphere, at least a moderate storm will follow.

2. Some of the correlations between solar and 1 AU properties reverse at solar minimum: (i) launch hemisphere with leading field of cloud, (ii) sigmoid shape with handedness of cloud.

3. The fact that the leading field of the clouds associated with sigmoids does reverse at solar minimum (point 2i) implies that the leading field is not simply that of the global solar dipole, which is the case for CMEs associated with filament disappearances on the quiet solar disc.

4. The CFR model correctly predicts the leading field 50% of the time. From the lack of success of the CFR model, one is forced to conclude that sigmoids themselves do not simply launch into space with all local flux-rope properties unchanged.

[34] Alternatively, eruptions of coronal sigmoids are due to a somewhat different mechanism to quiescent filament disappearances. A more basic distinction is that between an active region eruption (whether there is a sigmoid, a filament, or both) and a quiet-Sun eruption. A number of the events listed in Table 1 and studied here (including that illustrated in Figures 1 and 2) have both a sigmoid in the corona and a filament in the chromosphere. However, since sigmoids and filaments are both manifestations of non-zero helicity, and obey the same hemispheric handedness rules, we would be very surprised to see that in a given active region the handedness implied by the structures of filaments and sigmoids is different. Furthermore, the effects of the complex fields of active regions on their eruptive events are clearly not understood; loops and sigmoids above active regions do not necessarily connect the leader and follower polarities in a straightforward way. A simplistic classification of ARs by their leading polarity is probably inappropriate.

[35] Finally, we acknowledge the possibilities that the differences between eruptions before and after solar minimum is due to the decline or subsequent increase in solar activity, or somehow related to the ''Butterfly diagram'' progression of active regions to lower latitude. However, we believe that the best explanation to a dichotomous result is a dichotomous cause, namely the Hale cycle polarity reversal at solar minimum. Only observations for a full 22-year solar magnetic cycle can confirm or refute our conjecture.

[36] **Acknowledgments.** Yohkoh is a mission of ISAS in Japan; the SXT instrument is a collaboration of the University of Tokyo, the National Astronomical Observatory of Japan, and the Lockheed Martin Solar and Astrophysics Laboratory. The National Solar Observatory (NSO) is operated by the Association of Universities for Research in Astronomy (AURA, Inc.) under cooperative agreement with the National Science Foundation (NSF). NSO/Kitt Peak data used here are produced cooperatively by NSF/NOAO, NASA/GSFC, and NOAA/SEL. Interplanetary in situ data were provided by the NSSDC OMNIWeb database. We thank Isaac Klapper of the MSU Department of Mathematics for help with some of the statistical tests used here. Funding for this work was provided by AFOSR under grant number F49620-00-1-0128.

[37] Janet G. Luhmann thanks Volker Bothmer and David M. Rust for their assistance in evaluating this paper.

References

Amari, T., and J. F. Luciani, Confined disruption of a three-dimensional twisted magnetic flux tube, *Astrophys. J.*, *515*, L81, 1999.

Aulanier, G., and P. Démoulin, 3-D magnetic configurations supporting prominences, I, The natural presence of lateral feet, *Astron. Astrophys.*, *329*, 1125, 1998.

Aulanier, G., P. Démoulin, L. van Driel-Gesztelyi, P. Mein, and C. DeForest, 3-D magnetic configurations supporting prominences, II, The lateral feet as a perturbation of a twisted flux-tube, *Astron. Astrophys.*, *335*, 309, 1998.

Bothmer, V., and D. M. Rust, The field configuration of magnetic clouds and the solar cycle, in *Coronal Mass Ejections*, *Geophys. Monogr. Ser.*, vol. 99, edited by N. Crooker, J. A. Joselyn, and J. Feynmann, p. 139, AGU, Wasington, D.C., 1997.

Bothmer, V., and R. Schwenn, Eruptive prominences as sources of magnetic clouds in the solar wind, *Space Sci. Rev.*, *70*, 215, 1994.

Bothmer, V., and R. Schwenn, The structure and origin of magnetic clouds in the solar wind, *Ann. Geophys.*, *16*, 1, 1998.

Burlaga, L. F., E. C. Sittler, F. Mariani, and R. Schwenn, Magnetic loop behind an interplanetary shock: Voyager, Helios and IMP8 observations, *J. Geophys. Res.*, *86*, 6673, 1981.

Burlaga, L. F., et al., A magnetic cloud containing prominence material: January 1997, *J. Geophys. Res.*, *103*, 277, 1998.

Canfield, R. C., H. S. Hudson, and D. E. McKenzie, Sigmoidal morphology and eruptive solar activity, *Geophys. Res. Lett.*, *26*, 627, 1999.

Canfield, R. C., H. S. Hudson, and A. A. Pevtsov, Sigmoids as precursors of solar eruptions, *IEEE Trans. Plasma Sci.*, *28*, 1786, 2000.

Crooker, N. U., Solar and heliospheric geoeffective disturbances, *J. Atmos. Sol. Terr. Phys.*, *62*, 1071, 2000.

Gibson, S. E., and B. Low, 3-D and twisted: Magnetic field topologies of CMEs (SH41C-08), *Eos Trans. AGU*, *82*(20), Spring Meet. Suppl., SH41C-08, 2001.

Gonzalez, W. D., and B. T. Tsurutani, Criteria of interplanetary parameters causing intense magnetic storms (*Dst* of less than −100 nT), *Planet. Space Sci.*, *35*, 1101, 1987.

Gopalswamy, N., A. Lara, R. P. Lepping, M. L. Kaiser, D. Berdichevsky, and O. C. St. Cyr, Interplanetary acceleration of coronal mass ejections, *Geophys. Res. Lett.*, *27*, 145, 2000.

Gosling, J. T., Coronal mass ejections and magnetic flux ropes in interplanetary space, in *Physics of Magnetic Flux Ropes*, *Geophys. Monogr. Ser.*, vol. 58, edited by C. T. Russell, E. R. Priest, and L. C. Lee, p. 343, AGU, Washington, D.C., 1990.

Gosling, J. T., Corotating and transient solar wind flows in three dimensions, *Annu. Rev. Astron. Astrophys.*, *34*, 35, 1996.

Hale, G. E., and S. B. Nicholson, *Magnetic Observations of Sunspots, 1917–1924*, Carnegie Inst. of Wash., Washington, D.C., 1938.

Hudson, H. S., J. R. Lemen, O. C. St. Cyr, A. C. Sterling, and D. F. Webb, X-ray coronal changes during halo CMEs, *Geophys. Res. Lett.*, *25*, 2481, 1998.

Larson, D. E., et al., Tracing the topology of the October 18–20, 1995, magnetic cloud with $\sim 0.1-10^2$ keV electrons, *Geophys. Res. Lett.*, *24*, 1911, 1997.

Lepping, R. P., and D. Berdichevsky, Interplanetary magnetic clouds: Sources, properties, modeling and geomagnetic relationship, *Recent Res. Devel. Geophys.*, *3*, 77, 2000.

Lepping, R. P., J. A. Jones, and L. F. Burlaga, Magnetic field structure of interplanetary magnetic clouds, *J. Geophys. Res.*, *95*, 11,957, 1990.

Martin, S. F., and A. H. McAllister, Predicting the sign of magnetic helicity in erupting filaments and coronal mass ejections, in *Coronal Mass Ejections*, *Geophys. Monogr. Ser.*, vol. 99, edited by N. Crooker, J. A. Joselyn, and J. Feynmann, p. 127, AGU, Washington, D.C., 1997.

Martin, S. F., R. Bilimoria, and P. W. Tracadas, *Magnetic Field Configurations Basic to Filament Channels and Filaments*, p. 303, Kluwer Acad., Norwell, Mass., 1994.

Marubashi, K., Structure of the interplanetary magnetic clouds and their solar origins, *Adv. Space Res.*, *6*(6), 335, 1986.

Mehta, C. R., and N. R. Patel, A network algorithm for performing Fisher's exact test for $r \times c$ contingency tables, *J. Am. Stat. Assoc.*, *78*, 427, 1983.

Mulligan, T., C. T. Russell, and J. G. Luhmann, Solar cycle evolution of the structure of magnetic clouds in the inner heliosphere, *Geophys. Res. Lett.*, *25*, 2959, 1998.

Mulligan, T., C. T. Russell, and J. G. Luhmann, Interplanetary magnetic clouds: Statistical patterns and radial variations, *Adv. Space Res.*, *26*, 801–806, 2000.

Pevtsov, A. A., and R. C. Canfield, Solar magnetic fields and geomagnetic events, *J. Geophys. Res.*, *106*, 25,191, 2001.

Pevtsov, A. A., R. C. Canfield, and T. R. Metcalf, Latitudinal variation of helicity of photospheric magnetic fields, *Astrophys. J. Lett.*, *440*, 109, 1995.

Pevtsov, A. A., R. C. Canfield, and H. Zirin, Reconnection and helicity in a solar flare, *Astrophys. J.*, *473*, 533, 1996.

Pevtsov, A. A., R. C. Canfield, and S. M. Latushko, Hemispheric helicity trend for solar cycle 23, *Astrophys. J.*, *549*, L261, 2001.

Press, W. H., S. A. Teukolsky, W. T. Vetterling, and B. P. Flannery, *Numerical Recipes in FORTRAN 77*, 2nd ed., Cambridge Univ. Press, New York, 1992.

Rust, D. M., Helicity conservation, in *Coronal Mass Ejections*, *Geophys. Monogr. Ser.*, vol. 99, edited by N. Crooker, J. A. Joselyn, and J. Feynmann, p. 119, AGU, Washington, D.C., 1997.

Rust, D. M., A new paradigm for solar filament eruptions, *J. Geophys. Res.*, *106*, 25,075, 2001.

Rust, D. M., and A. Kumar, Helical magnetic fields in filaments, *Sol. Phys.*, *155*, 69, 1994.

Rust, D. M., and A. Kumar, Evidence for helically kinked magnetic flux ropes in solar eruptions, *Astrophys. J. Lett.*, *464*, 199, 1996.

Shimazu, H., and K. Marubashi, New method for detecting interplanetary flux ropes, *J. Geophys. Res.*, *105*, 2365, 2000.

Sterling, A. C., and H. S. Hudson, Yohkoh SXT observations of X-ray "dimming" associated with a halo coronal mass ejection, *Astrophys. J.*, *491*, L55, 1997.

Titov, V. S., and P. Démoulin, Basic topology of twisted magnetic configurations in solar flares, *Astron. Astrophys.*, *351*, 707, 1999.

Tsurutani, B. T., and W. D. Gonzalez, The interplanetary causes of magnetic storms, in *Magnetic Storms*, *Geophys. Monogr. Ser.*, vol. 98, edited by B. T. Tsurutani, W. D. Gonzalez, Y. Kamide, and J. K. Arballo, p. 77, AGU, Washington, D.C., 1997.

Webb, D. F., E. W. Cliver, N. Gopalswamy, H. S. Hudson, and O. C. St. Cyr, The solar origin of the January 1997 coronal mass ejection, magnetic cloud and geomagnetic storm, *Geophys. Res. Lett.*, *25*, 2469, 1998.

Webb, D. F., E. W. Cliver, N. U. Crooker, O. C. St. Cyr, and B. J. Thompson, Relationship of halo coronal mass ejections, magnetic clouds and magnetic storms, *J. Geophys. Res.*, *105*, 7491, 2000a.

Webb, D. F., R. P. Lepping, L. F. Burlaga, C. E. DeForest, D. E. Larson, S. F. Martin, S. P. Plunkett, and D. M. Rust, The origin and development of the May 1997 magnetic cloud, *J. Geophys. Res.*, *105*, 27,251, 2000b.

R. C. Canfield and R. J. Leamon, Department of Physics, Montana State University, Bozeman, MT 59717-3840, USA. (canfield@physics.montana.edu; leamon@physics.montana.edu)

A. A. Pevtsov, National Solar Observatory, Sunspot, NM 88349, USA. (apevtsov@nso.edu)